Effect of particle size on fracture toughness of epoxy resin filled with angular-shaped silica

Yoshinobu Nakamura, Miho Yamaguchi and Akiko Kitayama
Central Research Laboratory, Nitto Denko Corporation, Shimohozumi, Ibaraki, Osaka, 567, Japan

and Masayoshi Okubo and Tsunetaka Matsumoto
Department of Industrial Chemistry, Faculty of Engineering, Kobe University, Nada-ku, Kobe, 657, Japan
(Received 28 June 1990; revised 7 August 1990; accepted 17 August 1990)

The effect of particle size on the fracture behaviour of cured epoxy resin filled with angular-shaped silica was studied. Angular-shaped silica particles were prepared by crushing fused natural raw silica and were classified into six groups with different mean sizes ranging from 2 to 47 μm. Critical stress intensity factor (K_c) and critical strain energy release rate (G_c) of the cured epoxy resin filled with these silica particles were measured. Both K_c and G_c values increased with an increase in particle size of the silica. Scanning electron microscopic observations of crack tips and fractured surfaces showed that the damage zone was formed at the crack tip by particle fracture and by crack diverging. This phenomenon became more pronounced with increase in the particle size. The higher K_c and G_c values appear to be derived from the dispersion of the stress concentrated at the crack tip due to the crack diverging and from energy absorption due to the formation of a damage zone.

(Keywords: epoxy resin; fracture toughness; silica particle; strain energy; fractography; crack propagation)

INTRODUCTION

Epoxy resin is widely used for coatings, adhesives, casting, electrical insulator material and other applications. However, unsolved problems still remain in these applications. The main problem is low toughness[1]: cured epoxy resin is rather brittle with poor resistance to the propagation of cracks, derived from the internal stress generated by shrinkage in the cooling process from cure temperature to room temperature[2,3]. Much effort has been made to solve this problem.

In a series of investigations[4–9], we have been trying to reduce the internal stress generated in the cured epoxy resin. For this purpose, a two-phase structure was introduced, in which soft polymer particles were dispersed as domains (second phase) in the epoxy matrix. The relationship between the morphology of the two-phase structure and the internal stress was studied in cured epoxy resin modified with acrylic polymers. As a result, the effects of the domain size[4] and the domain–matrix interaction[5–9] on the reduction of the internal stress were clarified.

Many researchers[10–21] have improved the toughness of epoxy resins by the introduction of a two-phase structure with such soft domains, and proposed some toughening mechanisms based on fracture mechanics. On the other hand, it has been reported that the two-phase structure with rigid filler particles as the second phase is also useful for toughening cured epoxy resin[22–36]. Most of these studies were carried out using glass beads but a few studies were made using angular-shaped silica particles ranging from 60 to 300 μm in diameter[34]. Recently, cured epoxy resin filled with such silica particles ranging in size from <1 μm to ~ 100 μm were used as packaging materials for integrated circuits[37,38].

In this paper, we report the effects of particle size on the fracture and toughening of cured epoxy resin using angular-shaped silica particles with sizes ranging from 2 to 47 μm.

EXPERIMENTAL

Materials

The angular-shaped silica particles were prepared by crushing amorphous silica made by fusing natural raw quartz at 1900°C (RD-8, Tatsumori Ltd). The crushed particles were classified into six groups by air separation. Scanning electron microscope (s.e.m.) photographs of the classified silica particles are shown in *Figure 1*. *Figure 2* shows their size distribution curves obtained using a laser beam size distribution analyser (Granulométre 715 type, Cilas Alcatel). The particle sizes at which the accumulated distribution values reached 50% were defined as the mean particle size and are shown on the corresponding curves in *Figure 2*.

The epoxy resin used was bisphenol A type epoxy resin (Epikote 828, Shell Chemical Co.; equivalent weight per epoxy group, 190 ± 5; average molecular weight, 380). 1,2-Cyclohexanedicarboxylic anhydride and tri-n-butylamine were used as a hardener and an accelerator respectively, for curing the epoxy resin.

0032-3861/91/122221-09

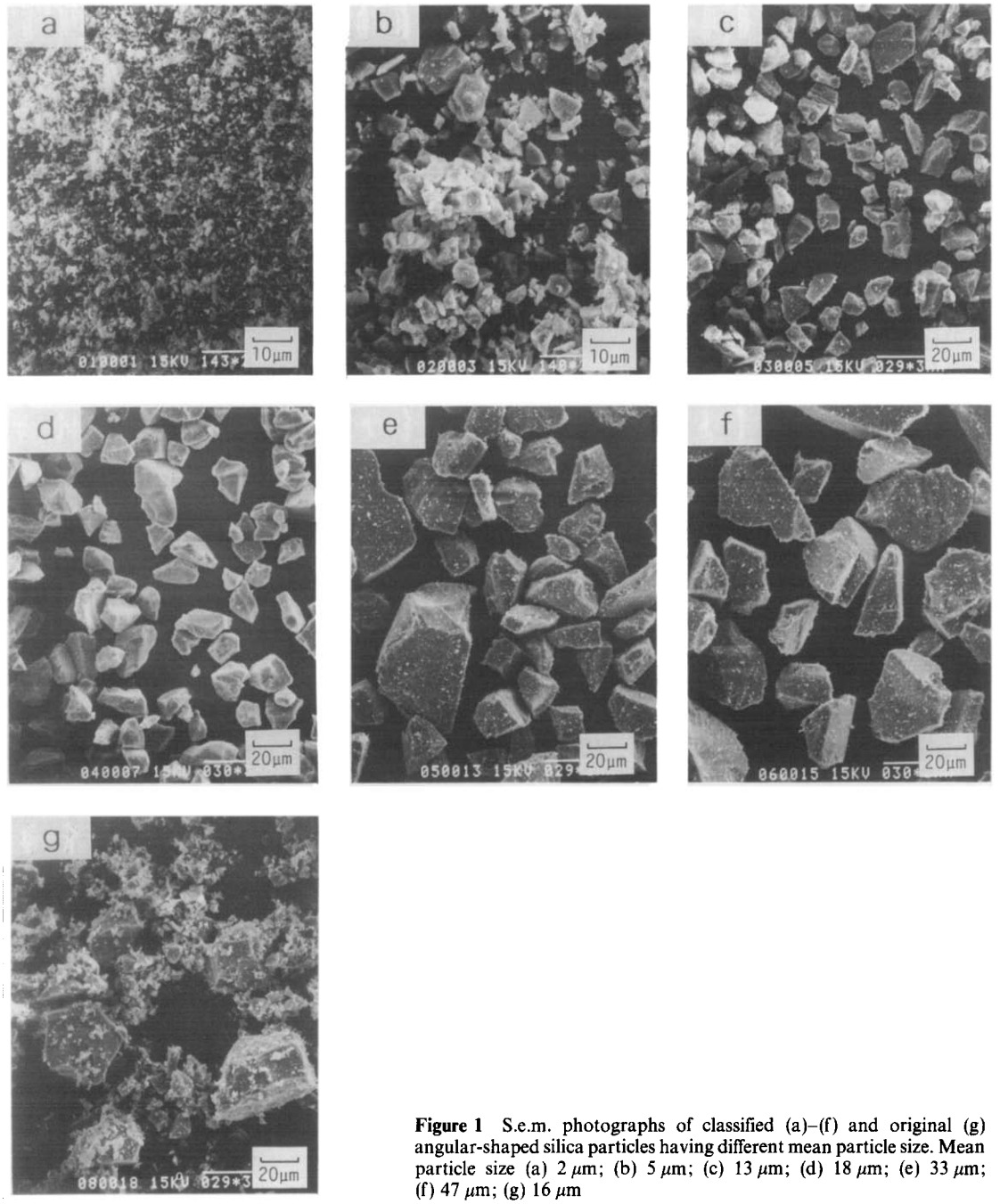

Figure 1 S.e.m. photographs of classified (a)–(f) and original (g) angular-shaped silica particles having different mean particle size. Mean particle size (a) 2 μm; (b) 5 μm; (c) 13 μm; (d) 18 μm; (e) 33 μm; (f) 47 μm; (g) 16 μm

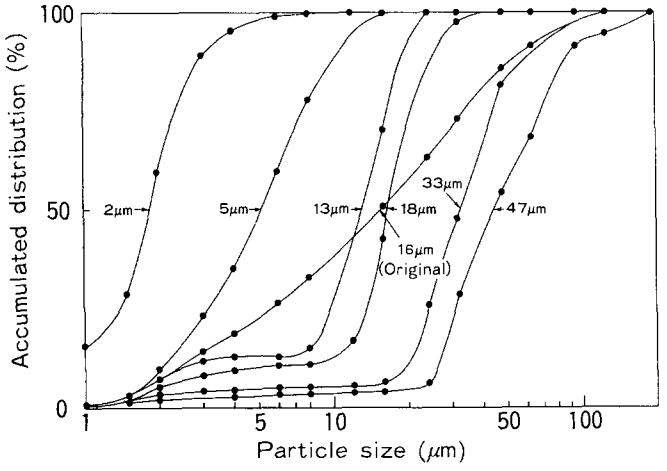

Figure 2 Accumulated particle size distribution curves for classified and original angular shaped silica particles. Mean particle size is indicated near curves

Sample preparation

Silica particles (204 or 296 parts per hundred parts of resin by weight (phr)) were dispersed in the mixture of epoxy resin (100 phr) and hardener (66 phr) at room temperature for 1 h while degassing in a vacuum. The accelerator (0.5 phr) was mixed with the mixture for 10 min. These procedures were carried out with stirring. The final mixture was cured in moulds ($4 \times 10\,mm^2$, height 100 mm and $4 \times 50\,mm^2$, height 140 mm) at 120°C for 2 h, followed by 140°C for 21 h.

Fracture studies

The critical stress intensity factor (or fracture toughness, K_c) and critical strain energy release rate (or fracture energy, G_c) were determined using a fracture mechanics technique[39]. The increase of K_c and G_c values indicates an increase of resistance to crack propagation[39].

In this study, K_c and G_c values were measured by single edge notched beam loaded in three point bending (SENB) fracture toughness test[40] and by double torsion (DT) fracture toughness test[30–32,40].

Single edge notched beam test. The shape and dimensions of the SENB test specimen are shown in *Figure 3*. Maintaining a temperature of 110°C, a sharp crack was introduced at the base of the slot in the test specimen using a fresh razor blade (Microtome knives, T-40 type, Nippon Microtome Laboratory Co. Ltd). Using an optical microscope it was seen that after the fracture test, a short starter crack was formed at the head of the initial sharp crack. The load *versus* time curve was recorded using a tensile testing machine (Tensilon UTM-5T type, Orientec Corp.) with a displacement rate of 10 mm min^{-1} at room temperature. The load increased linearly with time as shown in *Figure 3a*. When it reached the fracture load (P_c), the crack propagated, resulting in the fracture. The initial crack length (a), which is the sum of the length of the slot (b), the sharp crack (c) and the short starter crack (d) (see *Figure 3b*), of each fractured specimen was measured using an optical microscope.

The value of K_c was calculated from:

$$K_c = \frac{3P_cS}{2BW^2}(a)^{1/2}f(x) \quad (1)$$

where P_c is the load at fracture, a is the crack length, W is the specimen width, B is the specimen thickness, S is the support span and $f(x)$ is a geometric factor given by:

$$f(x) = 1.93 - 3.07x + 14.53x^2 - 25.11x^3 + 25.80x^4 \quad (2)$$

where $x = a/W$.

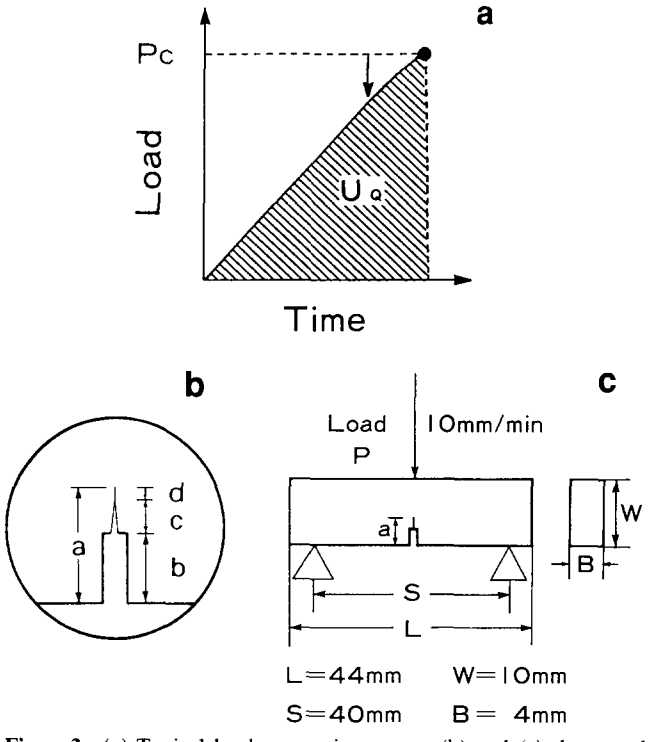

Figure 3 (a) Typical load *versus* time curve; (b) and (c) shape and dimension of SENB fracture toughness test specimen. The area of the crack is shown magnified in (b) where a = crack length; b = slot introduced by machining; c = sharp crack introduced by razor; d = starter crack. Arrow in (a) indicates the inflection point from elastic deformation

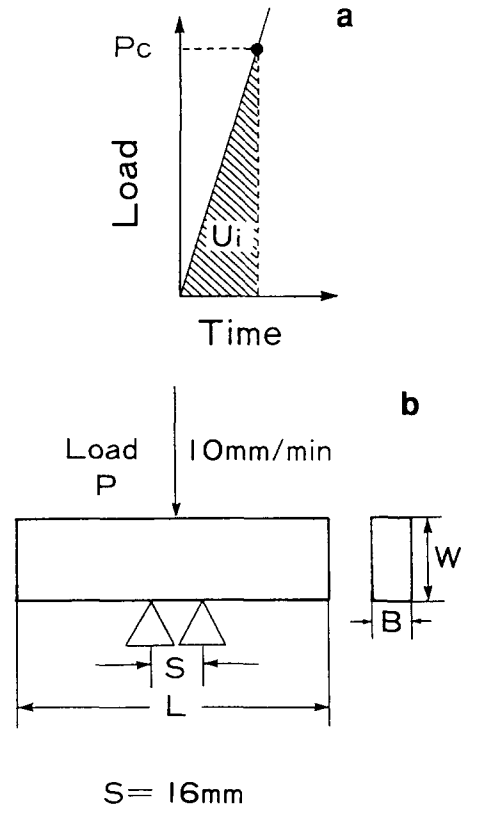

Figure 4 (a) Typical load *versus* time curve and (b) shape and dimension of indentation test specimen

The value of G_c was determined from the energy (U_Q) derived from integration of the load *versus* time curve (*Figure 3a*) as follows. For correcting the effects of loading pin penetration and specimen compression, the indentation test was also performed using a specimen without a slot under the narrow support span of 16 mm (see *Figure 4*). Using the energy (U_i) obtained from integration of the load *versus* time curve up to the same P_c value as that measured from the experiment shown in *Figure 3*, the true energy released by fracture (U) was calculated as follows:

$$U = U_Q - U_i \quad (3)$$

Using this U value, G_c was calculated from the following equations:

$$G_c = \frac{\eta_e U}{B(W-a)} \quad (4)$$

$$\eta_e = \frac{1-x}{\phi(x)} \quad (5)$$

$$\phi(x) = \frac{f^2(x)x\,dx}{f^2(x)x} + \frac{2}{9f^2(x)x} \quad (6)$$

$$f^2(x)x\,dx = 1.862x^2 - 3.95x^3 + 16.37x^4 - 37.22x^5 + 77.48x^6 - 126.8x^7 + 172.5x^8 - 143.9x^9 + 66.56x^{10} \quad (7)$$

This procedure is in accordance with ASTM[41,42] and other procedures[16,17].

Double torsion test. The shape and dimension of the specimen for the DT test are shown in *Figure 5*. The specimen had a notch and a V-shaped groove machined

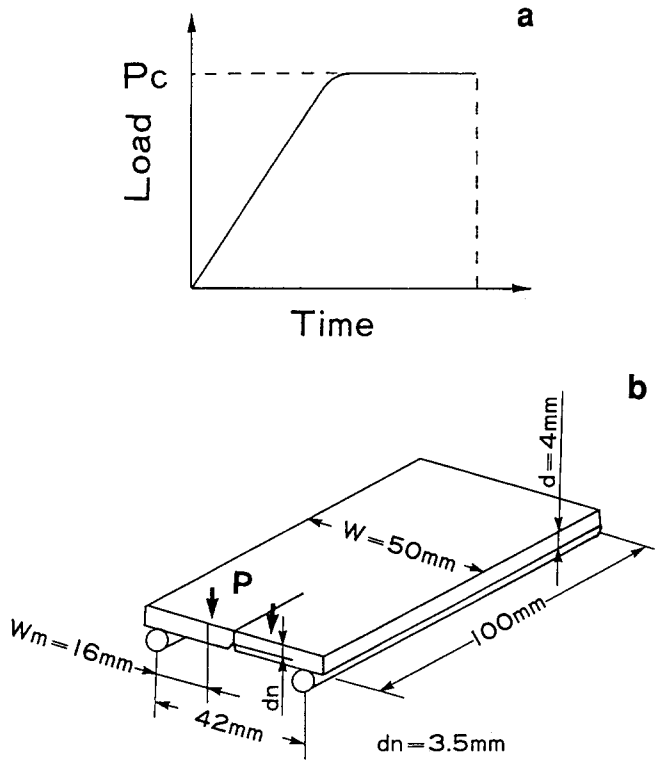

Figure 5 (a) Typical load *versus* time curve and (b) shape and dimension of DT fracture toughness test specimen. Arrows indicate direction of load

along the notch. A sharp crack was introduced at the base of the slot by the same method as described for the SENB test. The value of P_c was measured at a displacement rate of 0.5 mm min^{-1}. As shown in *Figure 5*, the load increased linearly and reached a constant value (P_c), i.e. the crack propagated stably along the centre shallow groove at a constant rate[30–32,40].

The value of K_c was calculated from:

$$K_c = P_c W_m \left[\frac{3}{W d^3 d_n (1-\nu)\xi}\right]^{1/2} \quad (8)$$

$$\xi = 1 - (5d/4W) \quad (9)$$

where P_c is the crack propagating load, W_m is the moment arm, W is the specimen width, d is the specimen thickness, d_n is the specimen thickness at the bottom of the groove, and ν is Poisson's ratio (=0.33).

G_c was calculated from:

$$G_c = \frac{K_c^2}{E}(1-\nu^2) \quad (10)$$

where E is the Young's modulus measured by a flexural technique. Discussion of measured E values is explained in detail elsewhere[43].

Fractography and observation for crack tip region

Figure 6a shows a schematic view of the original SENB specimen. The areas with bold outline in *Figure 6b–6d* show the parts observed by s.e.m. The starter crack tip region is shown in *Figure 6b*. Vertical views of the starter crack tip regions before and after the test were observed as shown in *Figure 6d* and *6c*, respectively. In both cases, the parts shown as broken lines were cut vertically and the exposed surfaces were polished with sand papers in the order of nos 200, 400, 800 and 1500 for 5 min each, followed by diamond powders of 1 μm and 3 μm for 15 min each in flowing water using an autopolishing machine (DAP-U type, Struers).

RESULTS AND DISCUSSION

Figure 7 shows the s.e.m. photographs of the polished surfaces of cured epoxy resins filled with the classified (*Figure 7a–f*) and original (*Figure 7g*) angular-shaped silica particles at a particle content of 55 wt%. These indicate that the particles were well dispersed in the cured epoxy matrix. In the resin containing the largest particles (*Figure 7f*), a difference in particle content between the upper and lower part of the specimen in the mould was observed, due to sedimentation of the particles during curing. However, since the particle contents of the fractured part of all specimens, obtained from the measurement of specific gravity, were almost equal to the particle contents in corresponding specimens, the effect of sedimentation was neglected.

Figures 8 and *9* show the effect of particle size on K_c and G_c values respectively, measured by the SENB test of the cured epoxy resin filled with silica particles. Values of K_c and G_c increased with increase in the particle size.

Figures 10 and *11* show the K_c and G_c values respectively, measured by the DT test. With increase in particle size, K_c and G_c values increased, as found for the SENB test (*Figures 8* and *9*). Values of K_c and G_c for 55 wt% particle content were larger than those for 64 wt% (see *Figures 8–10*), except in the case of the G_c

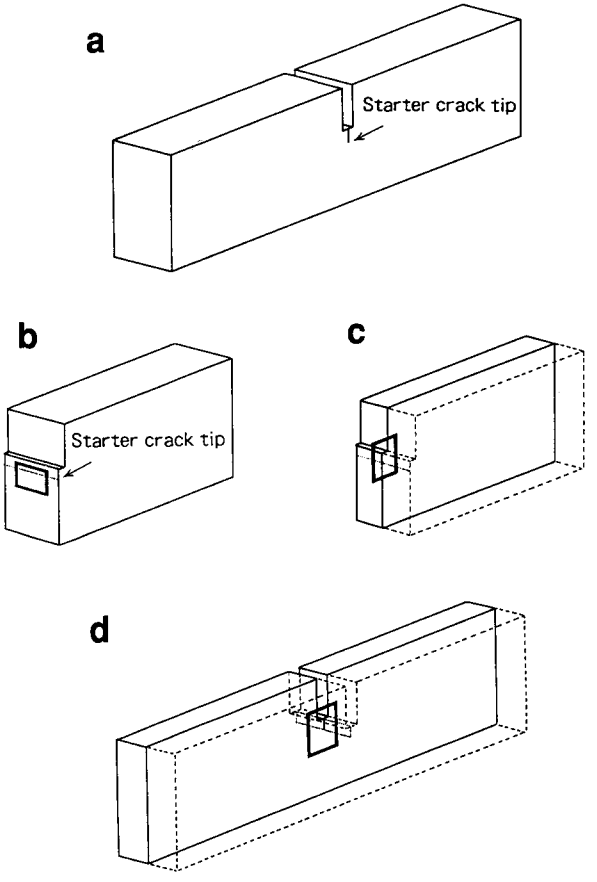

Figure 6 (a) Original SENB specimen; (b) fractured specimen after test; (c) vertically half cut fractured specimen after test; (d) vertically cut specimen before test. Areas with bold outline show parts observed by s.e.m.

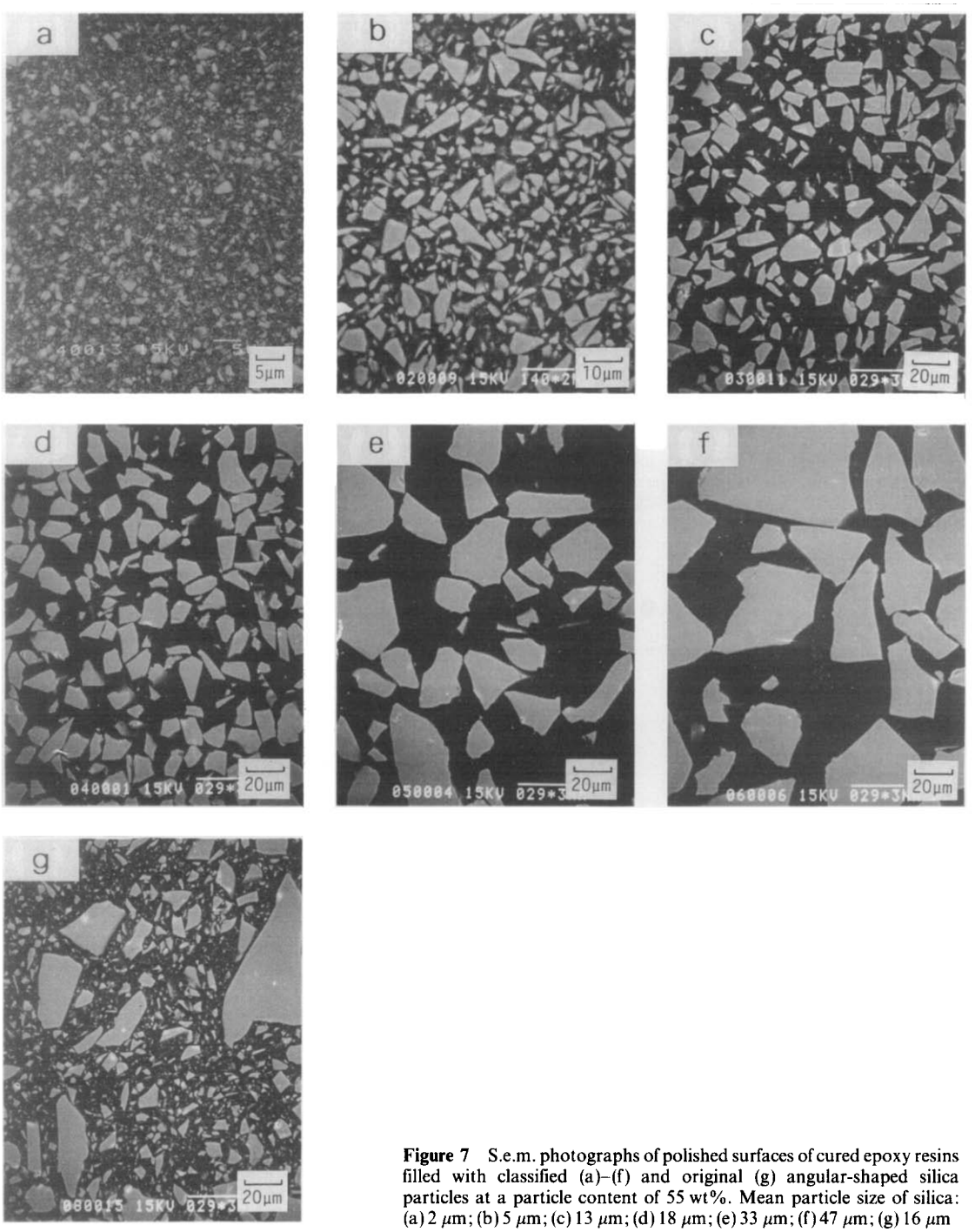

Figure 7 S.e.m. photographs of polished surfaces of cured epoxy resins filled with classified (a)–(f) and original (g) angular-shaped silica particles at a particle content of 55 wt%. Mean particle size of silica: (a) 2 μm; (b) 5 μm; (c) 13 μm; (d) 18 μm; (e) 33 μm; (f) 47 μm; (g) 16 μm

value obtained by the DT test (see *Figure 11*). The results obtained from *Figures 8–11* indicate that the addition of large angular-shaped silica particles increased the toughness of the cured epoxy resin. However, the degrees of increase of both K_c and G_c values with increase in particle size measured by the DT test (*Figures 10* and *11*) were smaller than those measured by the SENB test (*Figures 8* and *9*).

The fractured surfaces were then observed. It has already been reported that the slow propagating crack was observed ahead of the starter crack tip in the fractured SENB specimen[16,17], as shown schematically in *Figure 12*.

Figure 13 shows the regions around the starter crack tip front for surfaces of fractured SENB specimens observed by s.e.m. as shown in *Figure 6b*. The arrow in each photograph indicates the starter crack tip. In the unfilled cured epoxy resin (*Figure 13a*), the surface ahead of the starter crack tip was smooth. However, with addition of particles and increase in particle size (*Figure 13b* and *13c*), it became rougher and more irregular.

Figure 14 shows the s.e.m. photographs of the polished surfaces for the vertically cut fractured SENB specimens as shown in *Figure 6c*. The arrowhead in each micrograph indicates the starter crack tip. In the resin filled with small particles (mean size 5 μm, *Figure 14a*), the crack propagated almost linearly from the starter crack tip. However, in the resin filled with the largest particles (mean size 47 μm, *Figure 14b*), the crack propagated irregularly along the particles. This tendency was the same as that observed in *Figure 13*, and indicates that large particles obstruct the crack propagation.

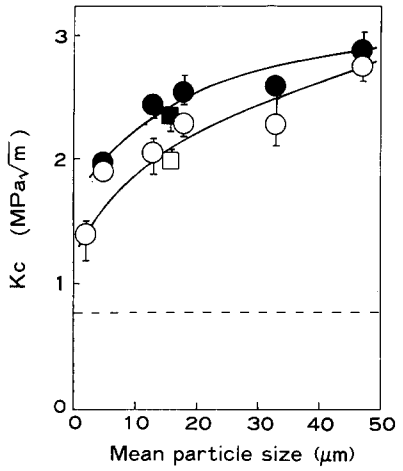

Figure 8 Effect of particle size on critical stress intensity factor (K_c) measured by SENB test of cured epoxy resins filled with original (□, ■) and classified (○, ●) angular-shaped silica particles at particle content of 55 wt% (□, ○) and 64 wt% (■, ●). Broken line indicates K_c value for unfilled cured epoxy resin

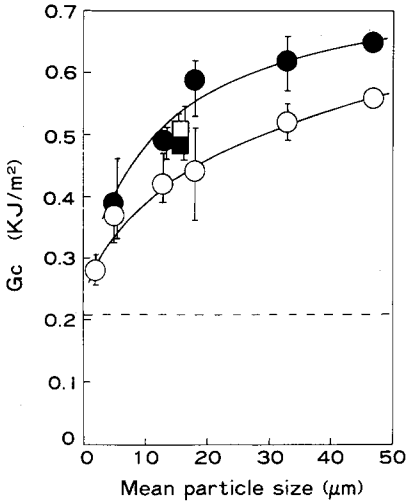

Figure 9 Effect of particle size on critical strain energy release rate (G_c) measured by SENB test of cured epoxy resins filled with original (□, ■) and classified (○, ●) angular-shaped silica particles at particle content of 55 wt% (□, ○) and 64 wt% (■, ●). Broken line indicates the G_c value for unfilled cured epoxy resin

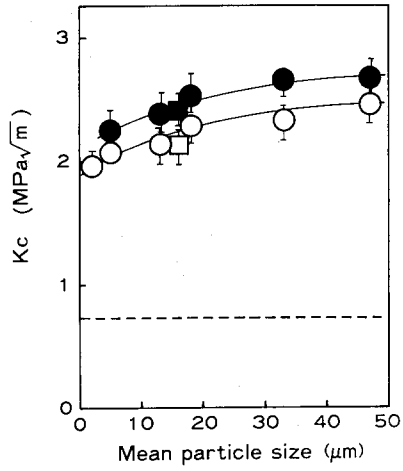

Figure 10 Effect of particle size on critical stress intensity factor (K_c) measured by DT test of cured epoxy resins filled with original (□, ■) and classified (○, ●) angular-shaped silica particles at particle content of 55 wt% (□, ○) and 64 wt% (■, ●). Broken line indicates the K_c value for unfilled cured epoxy resin

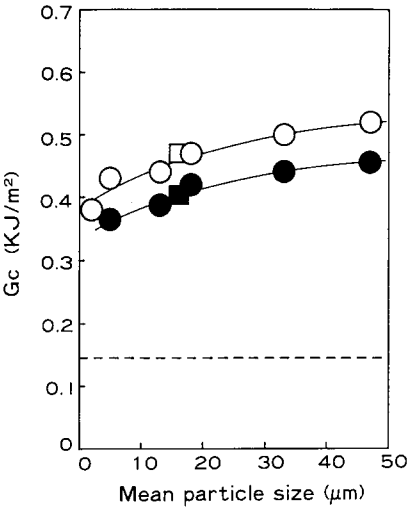

Figure 11 Effect of particle size on critical strain energy release rate (G_c) measured by DT test of cured epoxy resins filled with original (□, ■) and classified (○, ●) angular-shaped silica particles at particle content of 55 wt% (□, ○) and 64 wt% (■, ●). Broken line indicates the G_c value for unfilled cured epoxy resin

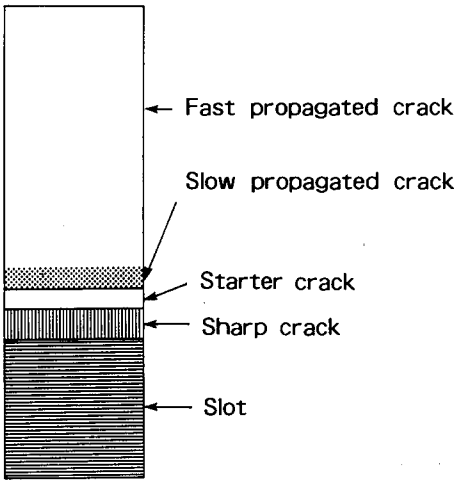

Figure 12 Schematic view of fractured surface of SENB specimen

Figure 15 shows the s.e.m. photographs of the starter crack tip region of the polished surfaces of vertically cut SENB specimens observed before test, as shown in *Figure 6d*. The magnified parts in *Figure 15b* and *15d* were from *Figure 15c* and *15e*, respectively. In the unfilled epoxy resin (*Figure 15a*), the starter crack tip was very sharp. In the resin filled with the small particles (*Figure 15b* and *15d*), it was also sharp, although slightly deflected by the particles. In the resin filled with the largest particles (*Figure 15c* and *15e*), however, it was not so sharp and was extensively deflected by the particles; some cracks in different directions were observed along the particle–matrix interface and in the fractured particles. These indicate that the starter crack, formed at the tip of the sharp crack introduced with the razor, was affected by the particle size. Since the divergence of the starter crack disperses the stress concentrated at the crack tip, greater energy is required for the initiating crack than for the sharp single crack. In the resin filled with the largest particles, some fractured particles were clearly observed, see *Figure 15d* and *15e*. As mentioned earlier, the silica

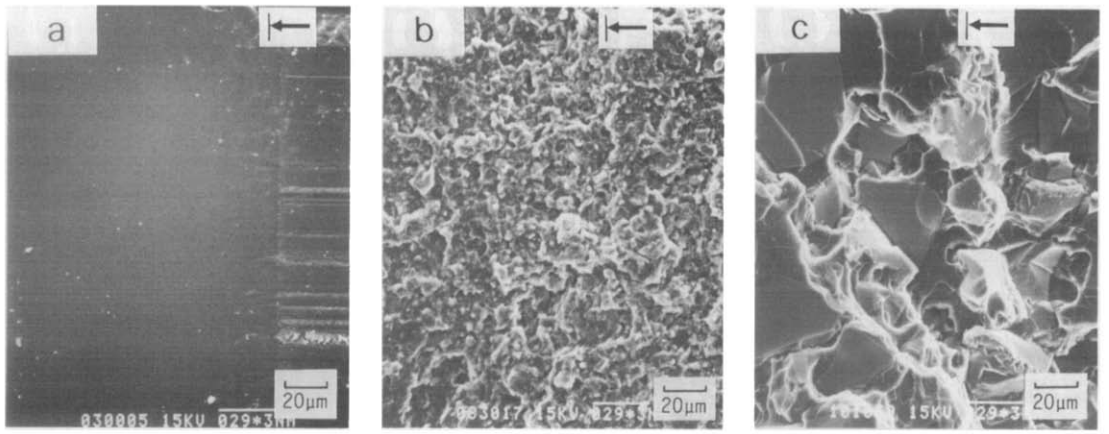

Figure 13 Regions around the starter crack tip front observed by s.e.m. for surfaces of fractured SENB specimens (see *Figure 6b*) of cured epoxy resins unfilled (a) and filled with angular-shaped silica particles (b) and (c) at particle content of 64 wt%. Mean particle size of silica: (b) 5 μm; (c) 47 μm. Arrow indicates the starter crack tip

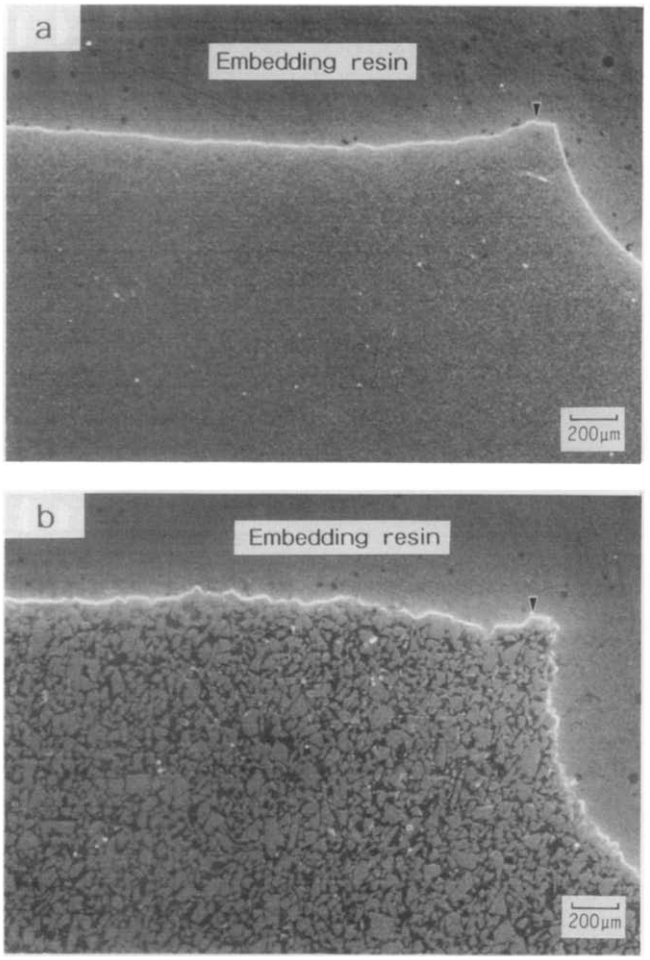

Figure 14 Polished surfaces observed by s.e.m. of vertically cut fractured SENB specimens (see *Figure 6c*) of cured epoxy resin filled with angular-shaped silica particles at particle content of 64 wt%. Mean particle size of silica: (a) 5 μm; (b) 47 μm. Arrowhead indicates the starter crack tip

particles were prepared by crushing fused raw silica. Therefore, with increasing particle size, the shape became more irregular and the number of cracks in the particles themselves increased (see *Figure 7*). This seems to be the reason for the fracture of particles.

In the SENB test, the inflection point from elastic deformation (see arrow in *Figure 3a*) was observed. Above this point, any energy absorption due to slow crack propagation or non-elastic deformation seems to be caused at the starter crack tip. To clarify this the crack tip region of the polished surfaces of vertically cut SENB specimens (as shown in *Figure 6d*) were loaded with 80% P_c, and observed by s.e.m. The resulting photographs are shown in *Figure 16*. The magnified parts in *Figure 16a* and *16c* were from *Figure 16b* and *16d*, respectively. In the resin filled with small particles (*Figure 16a* and *16b*), the observed crack tip was similar to its starter crack shown in *Figure 15b* and *15c*. In the resin filled with the largest particles (*Figure 16c* and *16d*), however, there were many cracks diverging in different directions along the particle–matrix interface and in the particles. Particle fractures were observed ahead of the starter crack tip region and this is termed the 'damage zone'[17,36] or 'process zone'[36]. In the resin filled with the largest particles (mean size 47 μm) it is clear that the damage zone was larger in the loaded specimen (*Figure 16c* and *16d*) than in the unloaded specimen (starter crack tip, *Figure 15d* and *15e*). However, in the resin filled with small particles (mean size 5 μm) the damage zone was not observed in either the unloaded (starter crack tip, *Figure 15b* and *15c*) or the loaded (*Figure 16a* and *16b*) specimens. The occurrence of microfracture in the damage zone should partially absorb the stored strain energy at the crack tip and suppress the crack propagation.

Figure 17 shows the load *versus* time curves for the DT test. In the resin filled with small particles (mean size 5 μm, *Figure 17a*), the load above the inflection point from elastic deformation decreased smoothly by a small amount. In the resin filled with the largest particles (mean size 47 μm, *Figure 17b*), however, it decreased unevenly resulting in the sawtooth shape of the curve. *Figure 17a* shows that the crack propagated continuously, while *Figure 17b* shows that the crack propagated with repeated initiation and arrest. With increasing particle size, the shape of the curve changed from *Figure 17a* to *17b* continuously. These results support the theory that suppression of crack propagation increases with increasing particle size.

On the basis of the above results, the effect of size of the filled angular shaped silica on toughness is schematically shown in *Figure 18*. In the resin filled with small particles (*Figure 18a*), the crack propagated linearly

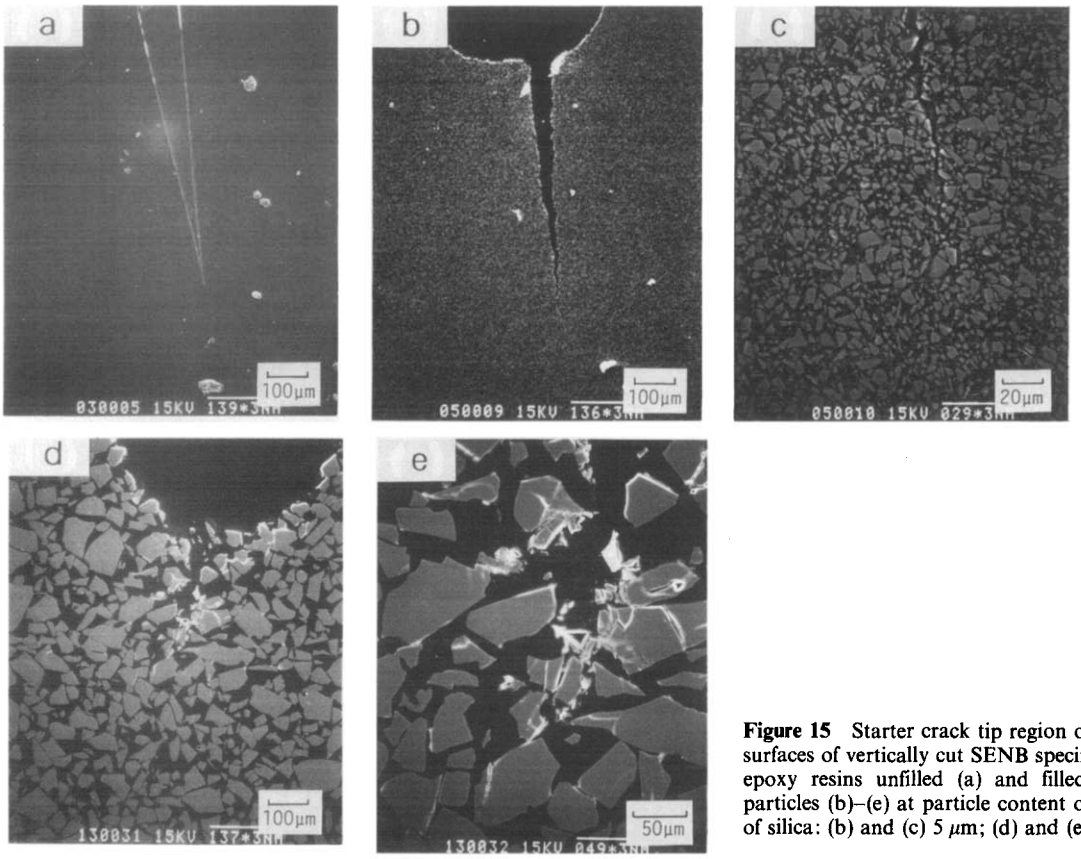

Figure 15 Starter crack tip region observed by s.e.m. of polished surfaces of vertically cut SENB specimens (see *Figure 6d*) of cured epoxy resins unfilled (a) and filled with angular-shaped silica particles (b)–(e) at particle content of 64 wt%. Mean particle size of silica: (b) and (c) 5 μm; (d) and (e) 47 μm

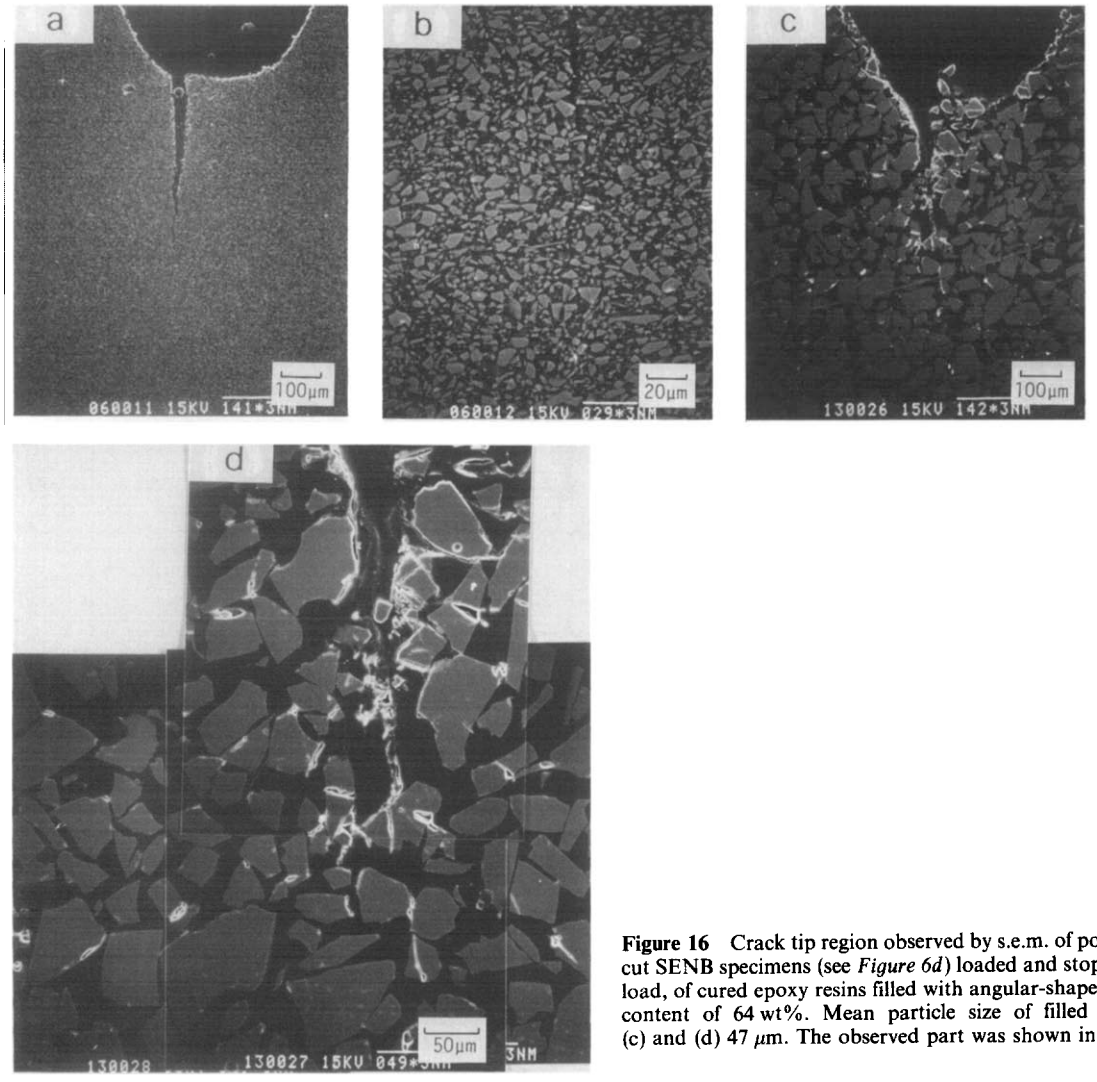

Figure 16 Crack tip region observed by s.e.m. of polished surfaces of vertically cut SENB specimens (see *Figure 6d*) loaded and stopped at 80% of the fracture load, of cured epoxy resins filled with angular-shaped silica particles at particle content of 64 wt%. Mean particle size of filled silica: (a) and (b) 5 μm; (c) and (d) 47 μm. The observed part was shown in *Figure 6d*

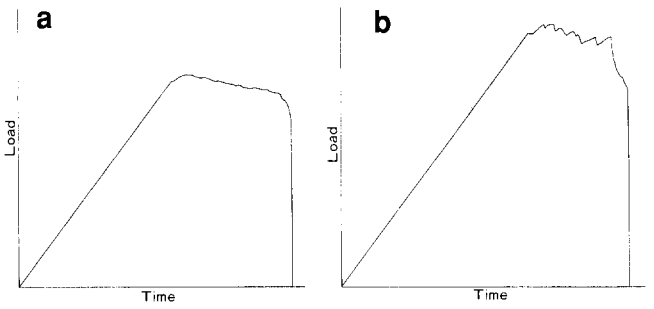

Figure 17 Load *versus* time curves for DT test of cured epoxy resins filled with angular-shaped silica particles at particle content of 55 wt%. Mean particle size of filled silica: (a) 5 μm; (b) 47 μm

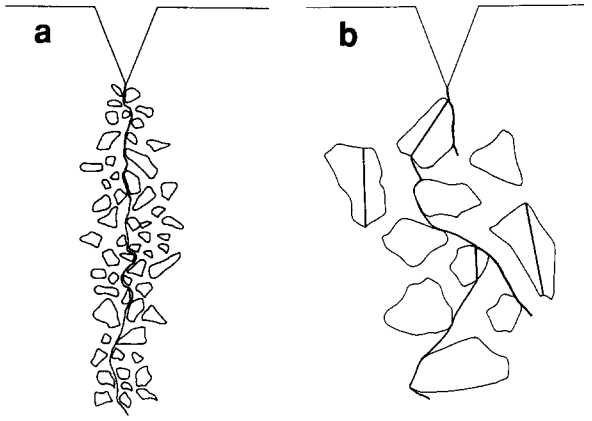

Figure 18 Schematic diagram of crack propagation mechanism of epoxy resins filled with (a) small and (b) large angular-shaped silica particles

although slightly deflected by the particles. In the resin filled with large particles (*Figure 18b*), however, the stress concentrated at the main propagating crack tip is dispersed and strain energy stored at the crack tip is partially released. This is due to obstruction of the main crack propagation in the slow propagating process and to formation of the damage zone at the main crack tip region due to the crack diverging and particle fracture. In addition to the size of particles, their shape may also affect toughness. In fact, the shape became more irregular with increase in particle size. In the above results, however, it is difficult to distinguish between the effects of particle size and shape on the toughness. In a future article, the effect of particle size on the toughness will be discussed using spherical silica particles.

As described above, the degrees of increase for both K_c and G_c values with increase in particle size were smaller when measured by the DT test than when measured by the SENB test. This may be because the effect of divergence of the starter crack on both K_c and G_c values is stronger in the SENB test than in the DT test.

In a subsequent article[43], the effect of particle size on mechanical properties will be discussed using the same silica particles.

ACKNOWLEDGEMENT

The authors are grateful to Tatsumori Ltd for the preparation of sample silica particles.

REFERENCES

1 Kinloch, A. J. and Young, R. J. 'Fracture Behaviour of Polymers', Elsevier Applied Science, London, 1983, p. 229
2 Shimbo, M., Ochi, M. and Arai, K. *J. Coat. Technol.* 1984, **56**, 45
3 Shimbo, M., Ochi, M. and Shigeta, Y. *J. Appl. Polym. Sci.* 1981, **26**, 2265
4 Nakamura, Y., Tabata, H., Suzuki, H., Iko, K., Okubo, M. and Matsumoto, T. *J. Appl. Polym. Sci.* 1986, **32**, 4865
5 Nakamura, Y., Tabata, H., Suzuki, H., Iko, K., Okubo, M. and Matsumoto, T. *J. Appl. Polym. Sci.* 1987, **33**, 885
6 Nakamura, Y., Yamaguchi, M., Kitayama, A., Iko, K., Okubo, M. and Matsumoto, T. *J. Appl. Polym. Sci.* 1990, **39**, 1045
7 Nakamura, Y., Yamaguchi, M., Iko, K., Okubo, M. and Matsumoto, T. *J. Mater. Sci.* 1990, **25**, 2711
8 Nakamura, Y., Yamaguchi, M., Iko, K., Okubo, M. and Matsumoto, T. *Polymer* 1990, **31**, 2066
9 Nakamura, Y., Yamaguchi, M., Iko, K., Okubo, M. and Matsumoto, T. *Kobunshi Ronbunsyu* 1990, **47**, 277
10 Sultan, J. N. and McGarry, F. J. *Polym. Eng. Sci.* 1973, **13**, 29
11 Bucknall, C. B. *Adv. Polym. Sci.* 1978, **27**, 121
12 Bascom, W. D., Cottington, R. L., Jones, R. L. and Peyser, P. *J. Appl. Polym. Sci.* 1975, **19**, 2545
13 Bascom, W. D., Ting, R. Y., Moulton, R. J., Riew, C. K. and Siebert, A. R. *J. Mater. Sci.* 1981, **16**, 2657
14 Kinloch, A. J., Shaw, S. J., Tod, D. A. and Hunston, D. L. *Polymer* 1983, **24**, 1341
15 Kinloch, A. J., Shaw, S. J. and Hunston, D. L. *Polymer* 1983, **24**, 1341, 1355
16 Yee, A. F. and Pearson, R. A. *J. Mater. Sci.* 1986, **21**, 2462
17 Pearson, R. A. and Yee, A. F. *J. Mater. Sci.* 1986, **21**, 2475; 1989, **24**, 2571
18 Kunz-Douglass, S., Beaumont, P. W. R. and Ashby, M. F. *J. Mater. Sci.* 1980, **15**, 1109
19 Sayre, J. A., Kunz, S. C. and Assink, R. A. *Am. Chem. Soc. Adv. Chem. Ser.* 1984, **208**, 215
20 Butta, E., Levita, G., Marchetti, A. and Lazzeri, A. *Polym. Eng. Sci.* 1986, **26**, 63
21 Garg, A. C. and Mai, Y.-W. *Compos. Sci. Technol.* 1988, **31**, 179
22 Moloney, A. C., Kausch, H. H., Kaiser, T. and Beer, H. R. *J. Mater. Sci.* 1987, **22**, 381
23 Faber, K. T. and Evans, A. G. *Acta Metall.* 1983, **31**, 565
24 Lange, F. F. *Phil. Mag.* 1970, **22**, 983
25 Evans, A. G. *Phil. Mag.* 1972, **26**, 1327
26 Green, D. J., Nicholson, P. S. and Embery, J. D. *J. Mater. Sci.* 1979, **14**, 1657
27 Broutsman, L. J. and Sahu, S. *Mater. Sci. Eng.* 1971, **8**, 98
28 Sahu, S. and Broutsman, L. *J. Polym. Eng. Sci.* 1972, **12**, 2, 97
29 Owen, A. B. *J. Mater. Sci.* 1979, **14**, 2523
30 Beaumont, P. W. R. and Young, R. J. *J. Mater. Sci.* 1975, **10**, 1334
31 Young, R. J. and Beaumont, P. W. R. *J. Mater. Sci.* 1975, **10**, 1343; 1977, **12**, 684
32 Spanoudakis, J. and Young, R. J. *J. Mater. Sci.* 1984, **19**, 473, 487
33 Su, K. B. and Suh, N. P. *Soc. Plastics Eng.* 1981, **27**, 46
34 Moloney, A. C., Kausch, H. H. and Stieger, H. R. *J. Mater. Sci.* 1983, **18**, 208
35 Moloney, A. C., Kausch, H. H. and Stieger, H. R. *J. Mater. Sci.* 1984, **19**, 1125
36 Narisawa, I. *Kobunshi Ronbunsyu* 1988, **45**, 683
37 Nakamura, Y., Uenishi, S., Kunishi, T., Miki, K., Kuwada, K., Tabata, H., Suzuki, H. and Matsumoto, T. *IEEE Trans. Components Hybrids Manuf. Technol.* 1987, **CHMT-12** (4), 502
38 Nishimura, A., Tatemichi, A., Miura, H. and Sakamoto, T. *IEEE Trans. Components Hybrids Manuf. Technol.* 1987, **CHMT-12** (4), 637
39 Kinloch, A. J. and Young, R. J. 'Fracture Behaviour of Polymers', Elsevier Applied Science, London, 1983, p. 74
40 Tait, R. B., Fry, P. R. and Garrett, G. G. *Exp. Mech.* 1987, **27**, 14
41 ASTM Committee D-20 on Mechanical Testing, Project No. X-10-128
42 ASTM E399-81
43 Nakamura, Y., Yamaguchi, M., Okubo, M. and Matsumoto, T. *J. Appl. Polym. Sci.* in press